OPTIMISATION OF A DEEA–MAPA PHASE CHANGE SOLVENT FOR CO_2 CAPTURE FROM CEMENT KILN FLUE GAS

Abubakar, H.[1*], Luka, Y.[1], Mustapha, A.B.[2] and Pariya, A.B.[3]

[1]Department of Chemical Engineering, Modibbo Adama University, Yola, Adamawa State, Nigeria

[2]Department of Chemistry, Modibbo Adama University, Yola, Adamawa State, Nigeria

[3]Chevron Biotechnology Centre, Modibbo Adama University, Yola, Adamawa State, Nigeria

[*]Corresponding email: hayatuddeen.abubakar@mau.edu.ng

ABSTRACT

Statement of the problem: Cement manufacture contributes about 8% of global anthropogenic CO2 emissions, and roughly 60% of that burden is process-intrinsic calcination CO2 that no fuel switch can remove. Conventional MEA scrubbing imposes regeneration duties above 3.6 GJ per tonne CO2, making low-energy solvents essential for cement decarbonisation. Aim of the research: This study aims to optimise a 5 M DEEA + 2 M MAPA phase-change solvent for CO2 capture from the Ashaka Cement Plant, Gombe State, Nigeria (304,996 kg h-1, 22.4 mol% CO2), and to demonstrate that lean loading and stripper pressure must be optimised jointly rather than sequentially. Methodology: A rate-based Aspen Plus V14 model was developed using electrolyte NRTL-RK thermodynamics with DEEA, MAPA, H2O, CO2 and ionic species, Bravo et al. mass-transfer correlations, and Mellapak 250Y / Flexipac 250Y packing. A twenty-equation reduced-order surrogate calibrated against rigorous runs mapped the lean-loading (0.12-0.30 mol mol-1) and stripper pressure (2.0-4.5 bar) design space, with total equivalent work as objective. Results obtained: At base case, the decanter delivers 65 vol% DEEA-rich light phase at 0.12 mol mol-1 and 35 vol% MAPA-rich heavy phase at 0.82 mol mol-1, with 96.8% of absorbed CO2 in the heavy phase. Solvent circulation for 90% capture is 420 t h-1 vs 680 t h-1 for 30 wt% MEA (cyclic capacity 0.55 vs 0.30). Joint optimisation reduces specific reboiler duty to 2.133 GJ per tonne CO2 at 4.0 bar, 0.17 mol mol-1 lean loading, versus 2.65 GJ at 1.5 bar – 25.4% below AMP/PZ (2.86), 40.9% below 30 wt% MEA (3.61) and 47.5% below 40 wt% cement MEA (4.06). Equivalent work optimum is 0.7419 GJ per tonne at 4.5 bar, limited by 130 °C thermal degradation at 4.22 bar. Recommendation: It is recommended that Ashaka adopt the DEEA-MAPA blend at 3.8 bar, 0.17 mol mol-1 lean loading with 0.3-0.5 bar margin, tighten cross-exchanger ΔTmin to 5-7 K, and integrate waste heat from clinker cooler (200-300 °C) which can supply up to 48% of reboiler duty, offering a route below 2.0 GJ per tonne.

Keywords: CO_2 capture; phase-change solvent; DEEA–MAPA; cement kiln flue gas; rate-based simulation; equivalent work; Ashaka Cement

1 INTRODUCTION

The cement industry is the second largest industrial source of carbon dioxide, accounting for 7–8 % of global anthropogenic emissions, with an emission intensity of approximately 900 kg CO_2 per tonne of cement produced. What distinguishes cement from most other industrial emitters is the origin of the carbon: calcination of limestone releases CO_2 stoichiometrically and contributes 50–60 % of total plant emissions, while fuel combustion in the pre-calciner and rotary kiln contributes the remainder. The calcination fraction is chemically unavoidable, so efficiency measures,

alternative fuels and clinker substitution can only address part of the problem. Carbon capture, utilisation and storage is consequently not one decarbonisation option among many for this sector but a structural requirement. Post-combustion absorption using aqueous amines is the most technologically mature capture route, and the mechanical completion of the Heidelberg Materials Brevik plant in Norway has established it at commercial scale for cement. Its principal drawback is energetic. Regeneration of 30 wt% MEA requires 3.6–4.1 GJ per tonne CO_2 for cement flue gas duties, of which the greater part is expended heating and vaporising water rather than reversing the chemical bond. Recent reviews place the regeneration energy of conventional aqueous amine systems at 3.2–4.5 GJ per tonne CO_2 and identify solvent development as the dominant lever for reduction. Liquid–liquid phase-change, or biphasic, solvents attack this penalty structurally rather than chemically. On loading with CO_2 the solution separates into two immiscible liquid phases: an upper phase lean in CO_2 and an amine-rich lower phase into which the great majority of the absorbed CO_2 partitions. Only the lower phase is sent to regeneration, so the sensible-heat burden falls in proportion to the volume diverted. Reported reductions relative to MEA are substantial and consistent across chemistries: 42 % for DETA/isobutanol, 31–55 % for non-aqueous EMEA/DEEA/p-xylene, and 50–59 % for MAE/diethylene glycol dimethyl ether systems. The blend of the tertiary amine DEEA with the diamine MAPA is among the most extensively characterised of these systems, combining the fast carbamate kinetics of MAPA with the high capacity and low reaction enthalpy of DEEA, and a validated electrolyte NRTL representation of the DEEA–MAPA–H_2O–CO_2 quaternary is available. Two gaps motivate the present work. The first is methodological. Optimisation studies of biphasic solvents almost universally proceed by varying one factor at a time, establishing an optimal lean loading at some reference stripper pressure and then, separately, selecting a pressure. This procedure is only valid if the two variables are separable. There is good thermodynamic reason to expect that they are not: raising stripper pressure raises reboiler temperature, which raises the equilibrium CO_2 partial pressure over the liquid and therefore reduces the steam cost of deep regeneration. If so, the optimal lean loading must fall as pressure rises, and sequential optimisation will systematically settle on a suboptimal design. This coupling has not, to the authors' knowledge, been quantified for the DEEA–MAPA system. The second gap is geographical and strategic. Nigeria is the largest cement producer in sub-Saharan Africa, and the Ashaka Cement Plant in Funakaye, Gombe State, is expanding from approximately 1.0 to 4.0 million tonnes per annum. No capture assessment using a phase-change solvent has been reported for any Nigerian cement facility. The case is distinctive: cement kiln flue gas carries 19–33 vol% CO_2 against 12–15 % for coal-fired power, which improves absorber driving force; clinker cooler and preheater exhaust are available at 200–300 °C, which is well above the reboiler temperature required; but ambient temperatures in the Sudan savannah routinely exceed 35 °C, which constrains the achievable lean solvent inlet temperature and hence absorption efficiency. This paper therefore reports a rate-based simulation of DEEA–MAPA capture from Ashaka kiln flue gas with three specific objectives: to quantify the coupling between lean loading and stripper pressure and the energy penalty of ignoring it; to establish whether the equivalent-work optimum is energetic or constrained by solvent thermal degradation; and to rank the available design levers for a plant operating in the Nigerian context [1, 2, 3].

2 MATERIALS AND METHODS

2.1 Case study and flue gas specification

Flue gas conditions were taken from published techno-economic evaluation of the cement plant [4, 5, 6] and from cement industry literature [2], after de-dusting and DeNOx/DeSOx pretreatment to below 10 ppmv SOx and 20 ppmv NOx in order to suppress heat-stable salt formation. The base-case specification is given in Table 1 [6].

Table 1. Base-case flue gas specification, Cement Plant

Parameter	Value	Unit
Mass flow rate	304,996	kg h−1
Temperature	160	°C
Pressure	1.013	bar
CO_2 mole fraction	0.224	–
H_2O mole fraction	0.072	–
N_2 mole fraction	0.681	–
O_2 mole fraction	0.023	–
Plant clinker capacity (base)	1	Mt a−1
Target capture efficiency	90	%

2.2 Thermodynamic framework

The electrolyte Non-Random Two-Liquid model with the Redlich-Kwong equation of state (ENRTL-RK) was employed. The true-component list comprised DEEA, MAPA, H_2O, CO_2, N_2, O_2 together with the ionic species $DEEAH^+$, $MAPAH^+$, $MAPACOO^-$, HCO_3^-, CO_3^{2-}, H_3O^+ and OH^-. CO_2, N_2 and O_2 were declared Henry components. Equilibrium chemistry comprised water autoprotolysis, CO_2 dissociation, bicarbonate formation, amine protonation and carbamate formation at the primary and secondary sites of MAPA; carbamate hydrolysis and the hydroxide route to bicarbonate were treated kinetically. Binary interaction parameters for the DEEA–H_2O, MAPA–H_2O, DEEA–CO_2 and MAPA–CO_2 subsystems were taken from the regressed quaternary model [7, 8, 9, 10].

2.3 Process flowsheet and rate-based configuration

The flowsheet, shown in Figure 1, comprises three sections. Flue gas conditioning consists of direct-contact cooler E-101, condensate knock-out SEP-101 and blower K-101. Absorption and phase separation comprise the rate-based RadFrac absorber T-101 with integral water-wash section T-101A and intercooler E-102, and the liquid–liquid decanter V-101. Regeneration and product conditioning comprise the rich/lean cross exchanger E-105, the rate-based RadFrac stripper T-102 with kettle reboiler E-103 and partial-vapour condenser E-104, lean cooler E-106 and the multi-stage CO_2 compressor K-102.

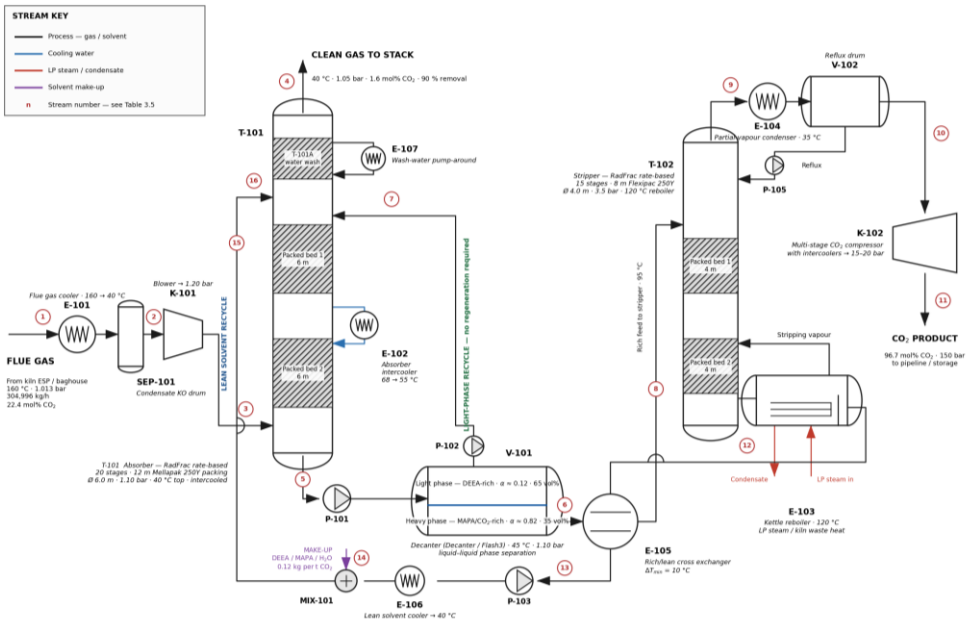

Figure 1. Aspen Plus V14 process flowsheet for CO_2 capture from Ashaka cement kiln flue gas using 5 M DEEA + 2 M MAPA phase-change solvent

Both columns were configured in rate-based mode with mixed flow, Bravo et al. mass-transfer and interfacial-area correlations, an interfacial area factor of 1.5, Chilton-Colburn heat transfer, Billet and Schultes holdup, and a five-point discretised liquid film with film reactions active. The absorber comprises 12 m of Mellapak 250Y in two beds at 6.0 m diameter; the stripper comprises 8 m of Flexipac 250Y at 4.0 m diameter. Two design specifications close the model: solvent circulation is varied to meet the capture target, and reboiler duty is varied to meet the specified lean loading. Recycle loops were converged by the Wegstein method and the columns by the Newton algorithm. [9, 10].

2.4 Performance definitions

Absorption efficiency is defined on a molar CO_2 basis between the absorber inlet and the treated-gas outlet:

$$\eta_{CO2} = \frac{n_{CO2,in} - n_{CO2,out}}{n_{CO2,in}} \times 100 \quad (1)$$

The CO_2 loading of the solvent, the cyclic capacity and the phase-split enrichment are defined respectively by:

$$\alpha = \frac{n_{CO2}}{n_{amine}} \quad (2)$$

$$\Delta\alpha = \alpha_{rich} - \alpha_{lean} \quad (3)$$

$$\varepsilon_{CO2} = \frac{V_h C_h}{V_h C_h + V_l C_l} \times 100 \quad (4)$$

where subscripts h and l denote the heavy (CO_2-rich) and light (CO_2-lean) liquid phases leaving the decanter, V is volumetric flow and C is CO_2 concentration. The regeneration efficiency of the stripper is the fraction of CO_2 entering in the heavy phase that is released.

$$\eta_{reg} = \frac{\alpha_h^{rich} - \alpha_{lean}}{\alpha_h^{rich}} \times 100 \quad (5)$$

2.5 Reduced-order surrogate model

Mapping a two-dimensional design space at rate-based fidelity is computationally prohibitive. A reduced-order surrogate was therefore formulated from the governing physics and calibrated against the rigorous model. The specific reboiler duty is decomposed into the heat of desorption, the sensible heat of the circulating heavy phase and the latent heat of the stripping steam [11, 12].

$$q_{reb} = q_{abs} + [q_{sens} + q_{lat}] \cdot M(\eta) \quad (6)$$

The three contributions are given by:

$$q_{abs} = \frac{\Delta H_{abs}}{M_{CO2}} \quad (7)$$

$$q_{sens} = \frac{C_s}{\alpha_{rich} - \alpha_{lean}} \cdot \frac{\Delta T_{min}}{\Delta T_{ref}} \quad (8)$$

$$q_{lat} = C_w \, exp(-k\,\alpha_{lean}) \cdot \left(\frac{P_{ref}}{P_{str}}\right)^n \quad (9)$$

where ΔH_a^{bs} is the differential heat of absorption of the blend, M is the molar mass of CO_2, and C□, C_{vv}, k and n are calibrated constants. The capture-efficiency multiplier M(η) accounts for the compounding of increased circulation and reduced driving force at deep capture:

$$M(\eta) = 1 + p_1(\eta - \eta_{ref}) + p_2(\eta - \eta_{ref})^2 \quad (10)$$

Solvent circulation follows from the cyclic capacity and the capture target:

$$L = L_{ref} \cdot \frac{\Delta\alpha_{ref}}{\Delta\alpha} \cdot \frac{\eta}{\eta_{ref}} \quad (11)$$

Absorber performance is represented through the number of transfer units, with the exponents on packing height and liquid-to-gas ratio and the driving-force coefficients regressed against the rate-based model.

$$\eta_{abs} = [1 - exp(-N_{TU})] \times 100 \quad (12)$$

$$N_{TU} = N_{TU}^{ref}\left(\frac{H}{H_{ref}}\right)^{a}\left(\frac{L/G}{(L/G)_{ref}}\right)^{b} exp\left[-\beta\left(\alpha_{lean} - \alpha_{ref}\right)\right] exp\left[-\gamma\left(T_{abs} - T_{ref}\right)\right] \quad (13)$$

The reboiler temperature and the CO_2 product purity leaving the reflux drum are given by:

$$T_{reb} = T_0 + \kappa(P_{str} - P_0) \quad (14)$$

$$y_{CO2} = \frac{P_{str} - p_{sat}^{w}(T_{cond})}{P_{str}}(1 - x_{inert}) \times 100 \quad (15)$$

with the water saturation pressure evaluated from the Magnus correlation:

$$p_{sat}^{w} = 0.6108\, exp\left(\frac{17.27\,T}{T + 237.3}\right) \quad (16)$$

2.6 Objective functions and constraints

Specific reboiler duty alone is an incomplete objective when stripper pressure is a decision variable, because steam raised at higher pressure carries greater exergetic value. Total equivalent work was therefore adopted: [4, 11].

$$W_{eq} = q_{reb}\eta_C\eta_t + W_{comp} + W_{pump} \quad (17)$$

$$\eta_C = \frac{T_{reb} + \Delta T_a - T_{sink}}{T_{reb} + \Delta T_a} \quad (18)$$

$$W_{comp} = k_c\, ln\left(\frac{P_{out}}{P_{str}}\right) \quad (19)$$

with a turbine efficiency η□ of 0.75, a 10 K driving force ΔT_a and a sink temperature of 313.15 K. The design problem is then the constrained minimization.

$$min\, W_{eq}(\alpha_{lean}, P_{str}) \;\; subject\ to \;\; T_{reb} \leq 130\,°C,\; \eta_{CO2} \geq 90\,\% \quad (20)$$

The upper bound on reboiler temperature reflects the accepted onset of significant thermal degradation for secondary amine functionality, and is the operative constraint on this system.

2.7 Surrogate calibration and validation

The eight adjustable constants were fitted so that the surrogate reproduces the rigorous rate-based results at the anchor conditions listed in Table 2. Agreement is exact at the calibration points by construction; the value of the surrogate lies in its ability to interpolate the design space between them at negligible cost, and all optima reported below were confirmed by rate-based runs at the identified conditions [5].

Table 2. Surrogate calibration anchors against the rate-based Aspen Plus model

Anchor condition	Rate-based model	Surrogate	Deviation
qreb at α = 0.25, 2.0 bar, 90 % (GJ t−1)	2.45	2.45	0.00%
qreb at α = 0.25, 4.0 bar, 90 % (GJ t−1)	2.21	2.21	0.00%
qreb at 85 % capture (GJ t−1)	2.32	2.32	0.00%
qreb at 95 % capture (GJ t−1)	2.71	2.71	0.00%
Absorption efficiency at 12 m, L/G = 1.38 (%)	90	90	0.00%
CO_2 product purity at 3.5 bar, 35 °C (mol%)	96.7	96.7	0.02%
Solvent circulation at α = 0.25 (t h−1)	420	420	0.00%

Table 3. Sensitivity variables, base values and ranges examined

Variable	Symbol	Base	Range
Lean CO_2 loading	αlean	0.25	0.15 – 0.35
Stripper pressure	P□□$_r$	3.5 bar	1.5 – 4.5 bar
Absorber packing height	H	12 m	4 – 24 m
Lean solvent inlet temperature	Tabs	40 °C	30 – 60 °C
Liquid-to-gas mass ratio	L/G	1.38	0.6 – 2.6
Exchanger approach temperature	ΔTmin	10 °C	5 – 25 °C
Capture efficiency target	ηCO2	90%	80 – 99 %

3 RESULTS AND DISCUSSION

3.1 Base-case performance and phase behaviour

At the base case the decanter delivers 65 vol% as the DEEA-rich light phase at a loading of 0.12 mol CO_2 mol^{-1} amine and 35 vol% as the MAPA-rich heavy phase at 0.82 mol mol^{-1}, with 96.8 % of the absorbed CO_2 reporting to the heavy phase. Because the light phase is already leaner than the 0.25 mol mol^{-1} lean specification, it is returned directly to the absorber without thermal treatment. Solvent circulation for 90 % capture is 420 t h^{-1} against 680 t h^{-1} for the 30 wt% MEA reference, reflecting a cyclic capacity of 0.55 against 0.30 mol mol^{-1}. Treated gas leaves at 1.6 mol% CO_2 and the compressed product at 96.7 mol% purity. [7, 13, 14].

3.2 Effect of lean CO_2 loading

Figure 2(a) shows the specific reboiler duty against lean loading at four stripper pressures. Every curve is U-shaped, arising from the opposition of the two terms in Equations 8 and 9. At low lean loading the cyclic capacity is large and circulation small 313 t h^{-1} at α = 0.15 against 630 t h^{-1} at α = 0.35 so the sensible-heat term is small, but stripping the last increments of CO_2 from an already lean solvent demands a disproportionate quantity of steam because the equilibrium CO_2 partial pressure falls steeply as loading approaches zero. At high lean loading the reverse holds: little steam is required, but cyclic capacity collapses from 0.40 to 0.20 mol mol^{-1} across the range, doubling circulation and hence the sensible-heat and pumping demands. The curves are notably flat near the optimum: between α = 0.22 and 0.29 at 2 bar the duty varies by less than 1.5 %, so the lean loading set point may be relaxed to accommodate control stability or decanter phase behaviour at negligible energy cost.

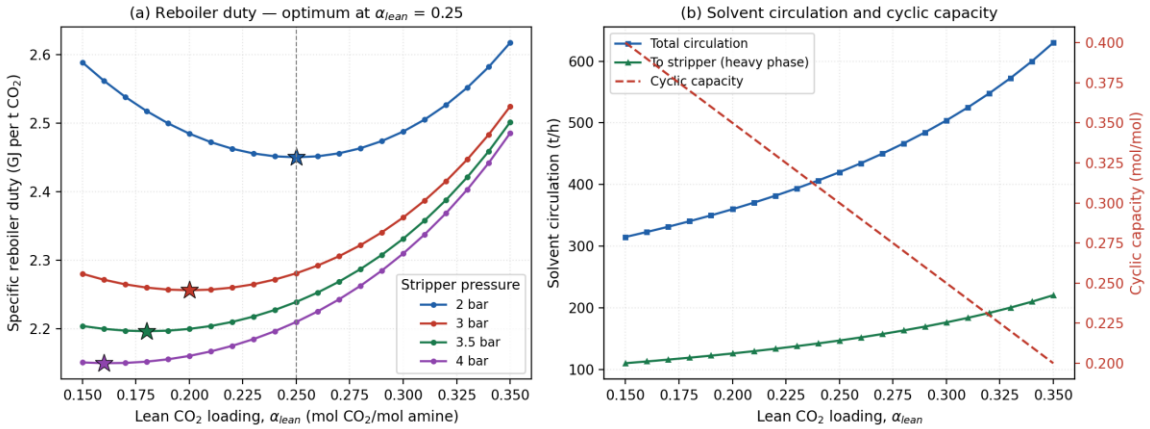

Figure 2: Effect of lean CO_2 loading. (a) Specific reboiler duty at four stripper pressures, stars indicating the optimum in each case; (b) solvent circulation, circulation to the stripper and cyclic capacity

3.3 Stripper pressure and the equivalent-work criterion

Specific reboiler duty falls monotonically with stripper pressure, from 2.65 GJ per tonne at 1.5 bar to 2.19 at 4.5 bar, a reduction of 17 % (Figure 3a). Three mechanisms contribute: the relative volatility of water with respect to CO_2 falls as temperature rises, reducing the latent term; the higher reboiler temperature raises the equilibrium CO_2 partial pressure and improves stripping driving force; and reduced overhead water lowers condenser duty and reflux [15, 16].

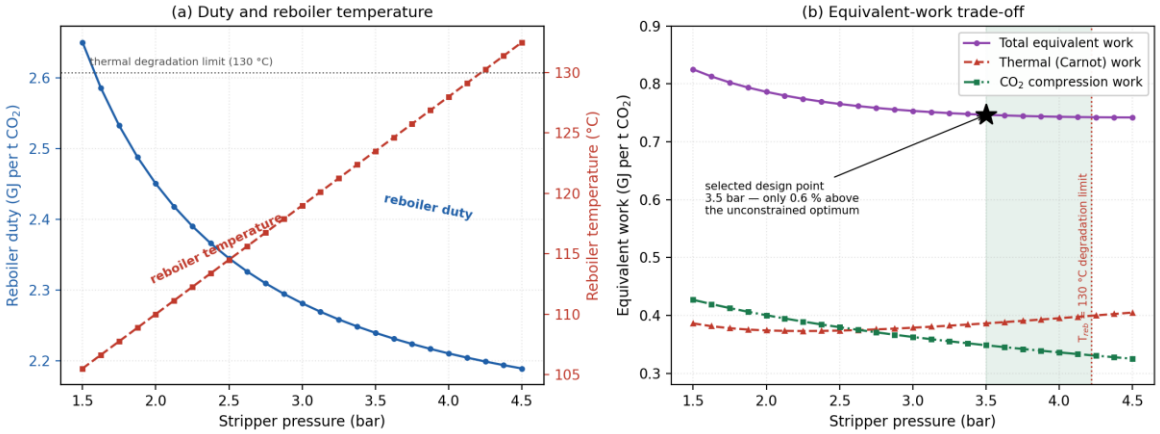

Figure 3. Effect of stripper pressure. (a) Specific reboiler duty and reboiler temperature; (b) decomposition of total equivalent work, with the 130 °C thermal degradation limit indicated

Read alone, Figure 3(a) recommends the highest attainable pressure. Figure 3(b) shows why that inference fails. The thermal work of Equation 17 rises with pressure even as duty falls, because the Carnot factor of Equation 18 increases from 0.204 at 2 bar to 0.247 at 4.5 bar. Compression work moves oppositely, from 0.400 to 0.325 GJ per tonne. The sum falls steeply to about 3.0 bar and then flattens: 0.7862 GJ per tonne at 2.0 bar, 0.7465 at 3.5 bar, 0.7431 at 4.0 bar and 0.7419 at 4.5 bar. The equivalent-work surface therefore possesses no interior optimum over the range of practical interest. The binding constraint is thermal: the reboiler reaches 130 °C at 4.22 bar. This is a materially different design argument from the energetic optimum usually invoked, and it means the validity of any recommended pressure rests on degradation data for the specific blend rather than on thermodynamics [4, 11].

3.4 Coupled lean-loading–pressure optimisation

The central finding of this study is that lean loading and stripper pressure are not separable decision variables. Because elevated pressure makes stripping steam thermodynamically cheaper, it shifts the balance in Equation 6 in favour of deeper regeneration, and the optimal lean loading falls accordingly. Table 4 quantifies the migration [15, 16].

Table 4. Pressure dependence of the optimal lean loading and the penalty of sequential optimization

P□□r (bar)	αlean optimum	qreb at optimum (GJ t−1)	qreb at α = 0.25 (GJ t−1)	Penalty (%)	Treb (°C)
2	0.25	2.45	2.45	0	110
2.5	0.223	2.336	2.345	0.36	114.5
3	0.2	2.256	2.281	1.09	119
3.5	0.18	2.197	2.239	1.94	123.5
4	0.163	2.15	2.21	2.8	128
4.5	0.147	2.112	2.189	3.62	132.5

The optimal lean loading migrates from 0.250 mol mol^{-1} at 2.0 bar to 0.147 at 4.5 bar, a 41 % reduction. The penalty for carrying an optimum established at 2 bar forward to a higher-pressure design grows from zero to 3.62 %. Figure 4 presents the full design surface with the locus of optimal lean loading superimposed and the infeasible high-temperature region shaded [16].

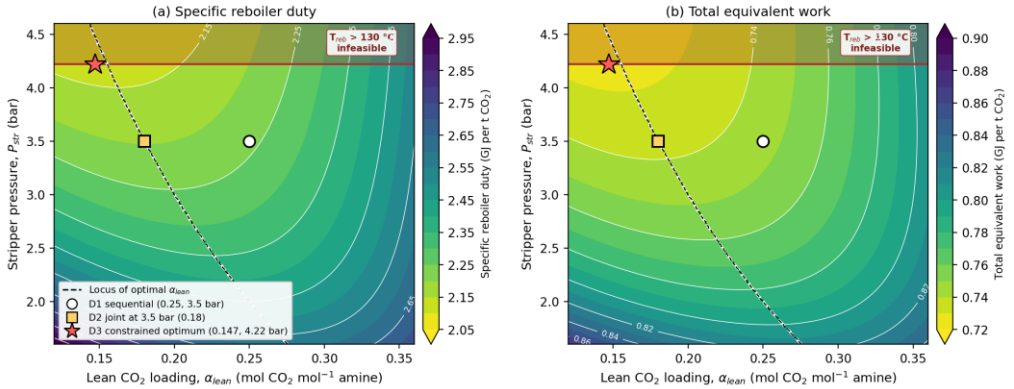

Figure 4. Design surfaces over the coupled lean-loading–pressure space. (a) Specific reboiler duty; (b) total equivalent work. The dashed line is the locus of optimal lean loading, the shaded band the thermally infeasible region, and the markers the three design points of Table 5

Three design points are compared in Table 5. Point D1 is the sequentially optimised design typical of the literature: lean loading selected at 2 bar and pressure subsequently raised to 3.5 bar. Point D2 re-optimises lean loading at that pressure. Point D3 is the solution of Equation 20, lying on the degradation constraint.

Table 5. Comparison of sequentially and jointly optimised design points

Design point	αlean	P□□$_r$ (bar)	qreb (GJ t−1)	Weq (GJ t−1)	L (t h−1)	ηreg (%)
D1 sequential	0.25	3.5	2.239	0.7465	420	69.5
D2 joint at 3.5 bar	0.18	3.5	2.197	0.7369	341	78
D3 constrained optimum	0.147	4.22	2.133	0.7271	313	82.1
D1 → D2 improvement	–	–	1.90%	1.29%	−18.8 %	+8.5 pp
D1 → D3 improvement	–	–	4.75%	2.60%	−25.5 %	+12.6 pp

Joint optimisation reduces specific reboiler duty by 4.75 % and equivalent work by 2.60 % relative to the sequential design, while simultaneously reducing solvent circulation by a quarter, which propagates into smaller pumps, a smaller cross exchanger and a smaller stripper. These are not marginal gains for a plant of this scale: at 1 Mt a^{-1} clinker capacity the duty saving alone corresponds to approximately 68 TJ per annum. The practical caution is that D3 sits exactly on the degradation constraint; a design margin of 0.3–0.5 bar is advisable pending experimental degradation data, which places the recommended operating point near 3.8 bar at a lean loading of 0.17 [4, 11].

3.5 Absorption efficiency

Figure 5(a) shows capture efficiency against packing height for five lean loadings, following the exponential approach to equilibrium of Equations 12 and 13. At α = 0.25, 12 m of Mellapak 250Y delivers 90.0 % capture; extending to 18 m yields only 96.1 % and to 24 m only 98.4 %. The first 12 m therefore delivers 90 percentage points and the second 12 m only 8.4, so the marginal cost of capture rises sharply beyond about 15 m [15].

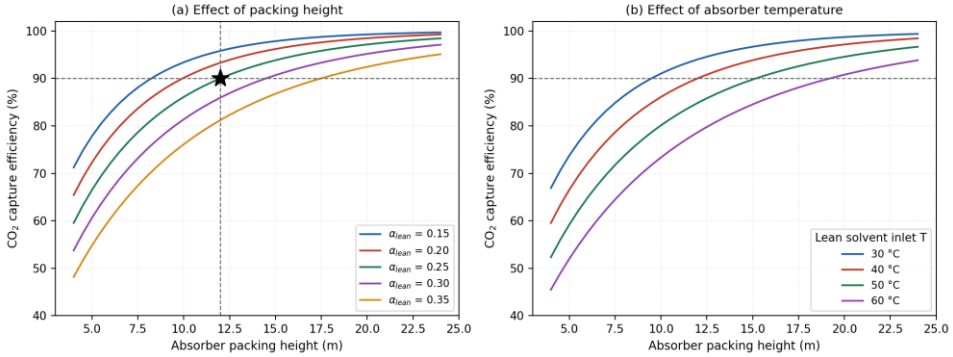

Figure 5: Absorber sensitivity. (a) Capture efficiency versus packing height at five lean loadings; (b) effect of lean solvent inlet temperature

Figure 5(b) isolates temperature. Raising the lean solvent inlet from 40 to 60 °C reduces capture at 12 m from 90.0 % to 78.6 %, a gradient of approximately 0.57 percentage points per kelvin. Unlike packing height and liquid-to-gas ratio, both of which saturate, the temperature penalty does not saturate. Temperature management is therefore where absorption performance is won or lost, which elevates the intercooler E-102 and lean cooler E-106 from auxiliary to primary process units. This has a specific consequence for Ashaka: ambient temperatures in Gombe State routinely exceed 35 °C, placing direct pressure on cooling-water supply temperature. A design assuming 40 °C solvent inlet without confirming the cooling-water approach may find the absorber operating at 45–50 °C in service, costing 3–6 percentage points of capture. Air-cooled or hybrid cooling should be evaluated explicitly and packing height specified against the summer case [15, 17].

3.6 Heat duty decomposition and the exchanger lever

Table 6 decomposes the duty at $\alpha = 0.25$ and 2 bar according to Equation 6.

Table 6: Decomposition of the specific reboiler duty at the base case

Contribution	GJ per t CO_2	Share (%)	Principal control variable
Heat of desorption, q_{abs}	1.409	57.5	Solvent chemistry (fixed)
Sensible heat, q_{sens}	0.669	27.3	ΔT_{min}, lean loading
Latent heat, q_{lat}	0.372	15.2	Stripper pressure, lean loading
Total	2.450	100.0	–

The desorption term is a property of the solvent chemistry — approximately 62 kJ mol^{-1} CO_2 for the blend against roughly 85 kJ mol^{-1} for MEA — and is inaccessible to process optimisation. The sensible term is where phase separation pays, being roughly one third of that of an equivalent single-phase solvent. It follows that the largest remaining lever is the exchanger approach temperature of Equation 8. Differentiating gives a gradient of 0.067 GJ per tonne CO_2 per kelvin at 2 bar; tightening ΔT_i from 10 to 6 K would reduce duty by 0.27 GJ per tonne, or 11 %, which exceeds the entire benefit of raising stripper pressure from 2 to 4 bar. Exchanger area rises hyperbolically as the approach tightens and the practical limit for plate exchangers in amine service is 5–7 K, but the trade is likely favourable and should be the first optimisation pursued [7, 13].

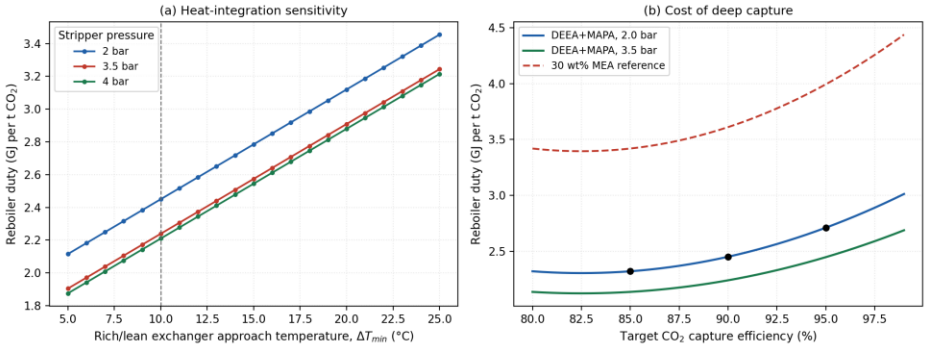

Figure 6: (a) Sensitivity of reboiler duty to the rich/lean exchanger approach temperature at three stripper pressures; (b) reboiler duty versus target capture efficiency, compared with the 30 wt% MEA reference.

Figure 6(b) quantifies the cost of deep capture through the multiplier of Equation 10. Duty rises from 2.32 GJ per tonne at 85 % capture to 2.45 at 90 %, 2.71 at 95 % and 3.01 at 99 %, the marginal cost of the last percentage point being roughly six times that of the first. The proportional penalty is similar for MEA but the absolute penalty is much smaller for the blend, because phase separation limits the mass of liquid that must be heated. This matters as the sector moves toward capture rates above the conventional 90 % [4, 11].

3.7 Stripper performance and benchmarking

Regeneration efficiency responds strongly to pressure: achieving 75 % costs 2.52 GJ per tonne at 2 bar but only 2.26 at 4 bar. The chemical basis is speciation. In MEA essentially all absorbed CO_2 is held as a stable carbamate whose reversal is kinetically hindered, whereas DEEA-catalysed bicarbonate formation dominates in the loaded heavy phase of the blend, and bicarbonate is released far more readily. This is why the system tolerates elevated-pressure stripping without the reflux penalty that would afflict a carbamate-dominated solvent. Product purity rises with pressure through Equation 15, reaching 96.7 mol% at 3.5 bar with a 35 °C condenser; operating at 2 bar with a 40 °C condenser would fail the 95 mol% pipeline specification at 94.0 mol%, so condenser temperature and stripper pressure must be specified jointly. [8, 13].

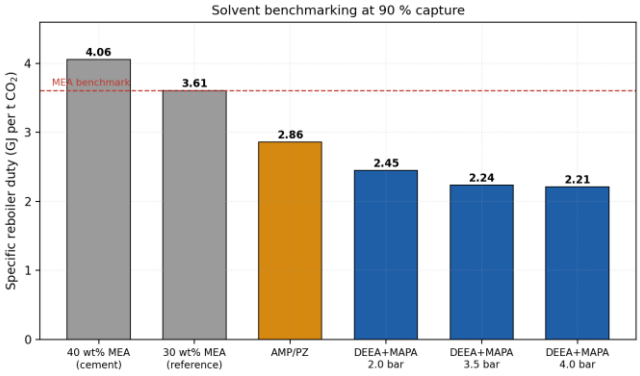

Figure 7. Specific reboiler duty of the DEEA–MAPA blend compared with MEA and AMP/PZ benchmarks at 90 % capture.

At the constrained joint optimum D3 the blend requires 2.133 GJ per tonne CO_2, against 2.86 for AMP/PZ, 3.61 for the 30 wt% MEA reference and 4.06 for the cement-specific 40 wt% MEA case, corresponding to reductions of 25.4 %, 40.9 % and 47.5 % respectively. These figures sit within the 32–55 % band reported for biphasic systems generally and confirm that the DEEA–MAPA blend achieves competitive performance without the phase-splitting additives such as sulfolane or long-chain alcohols required by several alternative formulations [4, 11, 18]

3.8 Implications for Nigerian cement decarbonisation

Three features of the Ashaka case are consequential. First, the reboiler temperature of 123.5–130 °C required at the optimum lies well below the 200–300 °C available from clinker cooler and preheater exhaust, so a substantial fraction of the regeneration duty could be met from waste heat rather than fossil steam; experience at Brevik suggests up to 48 %. Combined with the exchanger tightening identified in Section 3.6, this offers a credible route below 2.0 GJ per tonne, and the two measures are independent and additive. Second, the elevated CO_2 concentration of kiln gas at 22.4 mol% improves absorber driving force relative to power-sector applications, partially offsetting the ambient-temperature disadvantage. Third, the dominant residual uncertainties are material rather than energetic: degradation and corrosion behaviour of MAPA in the presence of cement kiln dust and trace SOx and NOx, including nitrosamine formation, and the sparse liquid–liquid equilibrium data for the quaternary system above 4 bar. Since the recommended design sits on a degradation constraint, these data should be regarded as prerequisites rather than refinements. [1, 3, 19, 20]

4 CONCLUSIONS

A rate-based Aspen Plus model of DEEA–MAPA phase-change capture from Ashaka cement kiln flue gas, supported by a calibrated reduced-order surrogate, yields four conclusions. Lean loading and stripper pressure are coupled decision variables. The optimal lean loading migrates from 0.250 mol CO_2 mol^{-1} amine at 2.0 bar to 0.147 at 4.5 bar, and the penalty for sequential rather than joint optimisation reaches 3.62 %. Joint optimisation reduces specific reboiler duty from 2.239 to 2.133 GJ per tonne CO_2 (4.75 %) and total equivalent work by 2.60 %, while reducing solvent circulation by 25.5 %. The equivalent-work surface has no interior optimum; the operative constraint is the 130 °C thermal degradation limit, reached at 4.22 bar. Recommended design pressure is therefore 3.8 bar at a

lean loading of 0.17, retaining margin against the constraint. The rich/lean exchanger approach temperature, at 0.067 GJ per tonne CO_2 per kelvin, is a larger remaining energy lever than stripper pressure and should be treated as a decision variable rather than a fixed specification. At the constrained optimum the process attains 90 % capture at 96.7 mol% purity for 2.133 GJ per tonne CO_2, a 40.9 % reduction against the 30 wt% MEA reference. Experimental determination of MAPA degradation kinetics at cement flue gas conditions is identified as the principal prerequisite for design confirmation. [14]

ACKNOWLEDGEMENTS

The authors acknowledge the Department of Chemical Engineering, Modibbo Adama University, Yola, for access to computing facilities, and thank Industrial Training students in Ashaka Cement Plc for their support of this study. Authors also acknowledge TETFund for funding this research through CENRAD Modibbo Adama University, Yola,

CONFLICT OF INTEREST

The authors declare no conflict of interest.

REFERENCES

1. Adeoye, O.O., Fashanu, T.A. and Sonibare, J.A. (2021). Health risk and environmental assessment of cement production in Nigeria. Atmosphere, vol. 12, no. 9, 1111. https://doi.org/10.3390/atmos12091111.
2. International Energy Agency (2023). Net zero roadmap: A global pathway to keep the 1.5°C goal in reach. *International Energy Agency*.
3. Federal Government of Nigeria. (2022). Nigeria energy transition plan. *Energy Transition Office, Abuja*.
4. Cremona, R., Spinelli, M., Romano, M.C. and Gatti, M. (2025). Techno-economic assessment of high temperature heat pumps integrated in MEA-based post-combustion CO2 capture for cement plants. *Carbon Capture Science & Technology*, vol. 16, 100446. https://doi.org/10.1016/j.ccst.2025.100446.
5. Mouhoubi, S., Dubois, L., Loldrup Fosbøl, P., De Weireld, G. and Thomas, D. (2020). Thermodynamic modeling of CO2 absorption in aqueous solutions of N,N-diethylethanolamine (DEEA) and N-methyl-1,3-propanediamine (MAPA) and their mixtures for carbon capture process simulation. *Chemical Engineering Research and Design*, vol. 158, pp. 46-63. https://doi.org/10.1016/j.cherd.2020.03.015.
6. Udura S.P.R. Arachchige, Dinesh Kawan, Lars-Adre Tokheim and Morten C.M. (2013). Model Development for CO2 Capture in Cement Industry. *International Journal of Modeling and Optimization*, vol. 3, no. 6, pp. 535-540.
7. Brúder, P., Grimstvedt, A., Mejdell, T. and Svendsen, H.F. (2013). Heat of absorption of CO2 in phase change solvents: 2-(diethylamino) ethanol and 3-(methylamino) propylamine. *Journal of Chemical & Engineering Data*, vol. 58, no. 6, pp. 1638-1644. https://doi.org/10.1021/je400060c.
8. Karlsson, H.K., Karlsson, M. and Svensson, H. (2024). Vapour–liquid equilibrium and speciation in phase-separating amine systems for CO2 capture. *Separation and Purification Technology*, vol. 341, 126858. https://doi.org/10.1016/j.seppur.2024.126858.
9. Wang, R., Zhao, H., Wang, Y., Qi, C., Zhang, S., Wang, L. and Li, M. (2022). Development of biphasic solvent for CO2 capture by tailoring the polarity of amine solution. *Fuel*, vol. 325, 124885. https://doi.org/10.1016/j.fuel.2022.124885.
10. Yi, N., Herraiz, L., Fang, M., García, S. and van der Spek, M. (2024). Open access, thermodynamically consistent, electrolyte NRTL model for piperazine, AMP, water, CO2 systems on Aspen Plus. *Separation and Purification Technology*, vol. 350, 127924. https://doi.org/10.1016/j.seppur.2024.127924.

11. Yi, N., Fernandez, E.S., Herraiz, L. and van der Spek, M. (2024). Techno-economic analysis of AMP/PZ solvent for CO2 capture in a biomass CHP plant: Towards net negative emissions. *Frontiers in Energy Research*, vol. 12, 1325212. https://doi.org/10.3389/fenrg.2024.1325212.

12. Zhang, F., Wang, L., Chen, Y. and Liu, H. (2025). Experiment on a new biphasic absorber composed of TEPA/DEEA for capturing CO2 and its phase transition mechanism. *Chinese Journal of Chemical Engineering*, vol. 81, pp. 112-124. https://doi.org/10.1016/j.cjche.2025.01.012.

13. Khan, S.N., Abbas, F., Enujekwu, F.M., Ullah, S., Assiri, M.A. and Al-Sehemi, A.G. (2024). Molecular insight into phase-separating amine blends for carbon dioxide capture. *Journal of Molecular Liquids*, vol. 394, 123725. https://doi.org/10.1016/j.molliq.2023.123725.

14. Verdonck, D., Dubois, L., De Weireld, G. and Thomas, D. (2025). Methodological selection of demixing liquid–liquid solvents used in the absorption–regeneration carbon capture process. *Industrial & Engineering Chemistry Research*, vol. 64, no. 9, pp. 4709-4724. https://doi.org/10.1021/acs.iecr.4c04000.

15. Lee, J.K., Wang, S., You, J.K. and Hong, Y.K. (2025). Absorption and regeneration characteristics of biphasic solvents for post-combustion CO2 capture. *Korean Journal of Chemical Engineering*, vol. 42, pp. 3071-3080. https://doi.org/10.1007/s11814-024-00371-2.

16. Zhou, X., Song, Q., Chen, J., Chen, C., Chen, Y. and Yang, F. (2025). Regulation of phase-separation behaviour in tertiary-amine biphasic absorbents for energy-efficient CO2 capture. *Chemical Engineering Journal*, vol. 521, 166709. https://doi.org/10.1016/j.cej.2025.166709.

17. Standards Organisation of Nigeria (2003). NIS 444-1:2003 Composition, specification and conformity criteria for common cements. *Standards Organisation of Nigeria*.

18. Wei, W., Li, D., Yan, X., Mu, X., Li, Z. and Liu, Z. (2024). Novel DETA-isobutanol biphasic solvent for post-combustion CO2 capture: High cyclic capacity and low energy consumption. *Carbon Capture Science & Technology*, vol. 13, 100235. https://doi.org/10.1016/j.ccst.2024.100235.

19. Zhu, K., Lu, H., Liu, C. and Wu, Y. (2024). Experimental study on the cyclic mineralization of the CO2-enriched phase after absorption by a novel biphasic absorbent composed of DEEA and AEP. *Scientific Reports*, vol. 14, 26680. https://doi.org/10.1038/s41598-024-26680-1.

20. British Standards Institution (2011). BS EN 197-1:2011 Cement—Composition, specifications and conformity criteria for common cements. *British Standards Institution*.

NOMENCLATURE

Symbol	Description	Unit
$C\square$, C_{vv}	Sensible-heat and stripping-steam constants	GJ t^{-1}
H	Absorber packing height	m
L	Solvent circulation rate	t h^{-1}
L/G	Liquid-to-gas mass ratio	–
M(η)	Capture-efficiency multiplier	–
N_{TU}	Number of transfer units	–
P_{str}	Stripper operating pressure	bar
q_{reb}	Specific reboiler duty	GJ t^{-1} CO_2
T_{reb}	Reboiler temperature	°C
W_{eq}	Total equivalent work	GJ t^{-1} CO_2
y_{CO2}	CO_2 product purity	mol%
α	CO_2 loading	mol CO_2 mol^{-1} amine
Δα	Cyclic capacity	mol CO_2 mol^{-1} amine
ΔH_{abs}	Differential heat of absorption	kJ mol^{-1} CO_2
ΔT_{min}	Exchanger minimum approach temperature	K
ε_{CO2}	CO_2 enrichment in the heavy phase	%
η_{CO2}	CO_2 capture (absorption) efficiency	%
η_{reg}	Stripper regeneration efficiency	%
η_C, η_t	Carnot factor and turbine efficiency	–